

Synthesis of Biocompatible Silver nanocubes

A dissertation submitted
for partial fulfillment for the requirement of
the award for the degree of

**Master of Science in
Physics**

Under the supervision of

Dr. B. N. Chudasama
(Assistant Professor)

Submitted by

Rajbir Singh
(301104012)



**School of Physics and Material Science
Thapar University,
(Formerly Thapar Institute of Engineering and Technology)
Patiala-147004, (Punjab) INDIA**

JULY - 2013

Dedicated To My

Respected

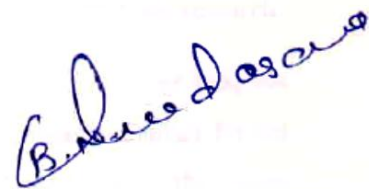
Parents

&

Teachers

Certificate

This is to certify that the report entitled “**Synthesis of Biocompatible silver nanocubes**” submitted by **Rajbir Singh** (Roll No. 301104012) of **M.Sc. Physics**, Thapar University, Patiala, was carried out under my supervision. The work presented in this thesis is his own work and is not credit towards any other degree at Thapar University, Patiala or any other University.



(Dr. B. N. Chudasama)
Research Supervisor
Thapar University,
Patiala.

Countersigned By:



(Dr. Kulvir Singh)
Professor & Head,
School of Physics & Material Science,
Thapar University, Patiala



(Dr. S. K. Mohapatra)
Dean of Academic Affairs,
Thapar University, Patiala.

Acknowledgement

First of all, I would like to thank **Dr.B.N.Chudasama**, my worthy supervisor, Assistant professor, School of Physics and Material Science, Thapar University, who has been an inspiration during my research work. Without him, this dissertation would not have been possible. I thank him for his patience and encouragement that carried me on through difficult times and for insight and suggestions that help to shape my research skills.

I also thank to **Dr. Kulvir Singh**, Professor and Head, School of Physics and Material Science for his support and for providing me infrastructural facilities to conduct this research.

A special thank to **Ms. Chandni Khurana, Ms. Parveer Kaur, Mr. Param jyot jha, Ms Ms. Pallvi Gupta, Ms. Shakshi Gupta and Mr. Satwinder Singh** research scholars for the help and valuable suggestions provided by them. Despite having a busy schedule they were always available for discussions and guidance. I am also thankful to my all classmates for their help and support during the course of this work. I owe my sincere gratitude to my family whose support and obstinate love gave me the energy to complete this dissertation work successfully and also for their untiring help during the difficult moment.

Rajbir Singh
15/7/13
Rajbir Singh

ABSTRACT

Over the last two decades the silver nanoparticles have elicited much interest. This is because these nanoparticles exhibit significantly novel physical, chemical and biological properties due to their nanoscale size. Nanostructured materials are attracting more attention because of their potential for achieving specific processes and selectivity, especially in biological and pharmaceutical applications. Silver nanoparticles (AgNPs) are already being used in numerous consumer products including textiles, food storage containers, water purification, home appliances, electronics, medical uses, catalyst, sensor and even food supplements. AgNPs are added to all these products because of their bactericidal and antimicrobial effects. In the present work, silver nanocubes have been prepared by polyol process by using chemical reduction method. Formation of silver nanocubes is confirmed by UV–vis spectroscopy, X-ray diffraction (XRD), transmission electron microscopy (TEM), Dynamic light scattering (DLS), thermogravimetric analysis (TGA). Hydrodynamic size of silver nanocubes was observed to be 36.4 ± 0.16 nm with polydispersity index of 0.5. The average crystallite size of the silver nanoparticles obtained from the peak broadening of diffraction peak was 9.38 nm. UV-Visible spectrum of the sample, hints towards the cubic shape of the silver nanoparticles, which is further confirmed by transmission electron microscopy. The presence of PVP coating is confirmed through TG analysis. This coating of PVP prevents the agglomeration of nanoparticles.

CONTENTS	PAGE NUMBER
Certificate	i
Acknowledgement	ii
Abstract	iii
List of figures	vi
List of tables	vi
CHAPTER 1 Introduction	1
1.1 Nanotechnology	1
1.2 Nano and bulk materials	1
1.3 Nobel metal nanomaterials (NMNs)	2
1.4 Silver	2
1.5 Silver nanoparticles	3
1.6 Applications of silver nanoparticles	3
1.6.1 Catalyst	4
1.6.2 Textile industry	4
1.6.3 Medical uses	4
1.6.4 Water purification	4
1.6.5 Sensor	4
1.6.6 Electronics	5

1.6.7 Other useful applications	5
CHAPTER 2 Literature Review	6
2.1 Synthesis of nanomaterials	6
2.1.1 Top-down approach	7
2.1.2 Advantages and disadvantages of Top-down approach	7
2.1.3 Bottom-up approach	7
2.1.4 Advantages and disadvantages of Bottom-up approach	8
2.1.5 Difference between Top-down and Bottom-up approach	8
CHAPTER 3 Experimental Techniques	14
3.1 Synthesis Method	14
3.2 Materials	15
3.3 Synthesis of silver nanocubes	15
3.4 Characterization Techniques	16
3.4.1 UV-visible Spectroscopy	16
3.4.2 X-Ray Diffraction (XRD)	18
3.4.3 Transmission electron microscope (TEM)	20
3.4.4 Dynamic light scattering (DLS)	22
3.4.5 Thermo Gravimetric analysis (TGA)	24
CHAPTER 4 Results and Discussion	27
4.1 UV-Visible Spectroscopy	27
4.2 X-Ray Diffraction (XRD)	28

4.3 Transmission electron microscope (TEM)	30
4.4 Dynamic Light Scattering (DLS)	31
4.5 Thermo Gravimetric analysis (TGA)	31
CONCLUSION	32
References	33

LIST OF FIGURES

Figure 2.1: Schematic representation of the building up of nanostructures.	6
Figure 3.1: Experimental Setup used for the synthesis of Ag nanocubes.	16
Figure 3.2: Schematic ray diagram of UV visible spectrophotometer.	18
Figure 3.3: Principle of X-ray diffraction.	19
Figure 3.4: Schematic ray diagram of TEM.	22
Figure 3.5: Brookhaven's 90 plus particle size analyzer.	23
Figure 3.6: Schematic diagram of particle size analyzer.	24
Figure 3.7: NETZSCH TGA/DTA thermal analyzer.	25
Figure 4.1: UV- visible spectra of Ag nanocubes.	27
Figure 4.2: X-ray diffraction pattern of silver nanocubes.	28
Figure 4.3: TEM image of silver nanocubes inset shows the electron diffraction images of Ag nanocubes.	30
Figure 4.4: Hydrodynamic size distribution of silver nanocubes.	31

Figure 4.5: TG curve of Ag nanocubes.

32

LIST OF TABLES

Table 4.1: Crystallite size obtained from various diffraction peaks.

29

Table 4.2: Calculated d-spacing corresponding to each Bragg's reflection.

29

Table 4.3: Lattice parameter of silver nanocubes.

29

1.1 Nanotechnology

Nanotechnology deals with various structures of matter having dimensions of the order of a billionth of a meter [1]. Nanotechnology manipulates matter at the atomic, molecular and macromolecular level. It aims at fabricating novel materials, devices and systems that have new properties and functions because of their small size [2]. It deals with materials having at least one dimension between 1 to 100 nm and involves developing materials or devices within that size [3].

We are interested in the nanoscale because materials reduced to the nanoscale can show different properties compared to what they exhibit on a macro scale, enabling unique applications. Matter such as gases, liquids, and solids can exhibit unusual physical, chemical, optical and biological properties at the nanoscale. For instance, opaque substances become transparent (copper); insoluble materials become soluble (gold), etc. Some materials at nanoscale are stronger or have different magnetic properties compared to bulk. Much of the fascination with nanotechnology stems from these quantum and surface phenomena that exhibits at the nanoscale [4]. Nanoparticles made from metals, semiconductors, or oxides are of particular interest for their mechanical, electrical, magnetic, optical, chemical and other properties.

1.2 Nano and bulk materials

- (1) Nanotechnology involves designing and producing objects or structures at a very small scale, on the level of 100 nm or less. Bulk particles are larger in the micron size range or even bigger.
- (2) Nanoparticles are so small that their physical properties are not constant over their size. They are of great scientific interest as they are effectively a bridge between bulk materials and atomic or molecular structures. A bulk material has constant physical properties regardless of its size.
- (3) The properties of materials change as their size approaches the nano-scale due to the increase in percentage atoms on the surface of the material. For bulk materials, larger than one micrometer, the percentage atoms on the surface of are very small relative to the total number of atoms of the material.

(4) Nanoparticles often have unexpected optical properties because they are small enough to confine their electrons and produce quantum effects.

(5) Nanoparticles have very high surface to volume ratio, which provides a tremendous driving force for diffusion, especially at elevated temperatures.

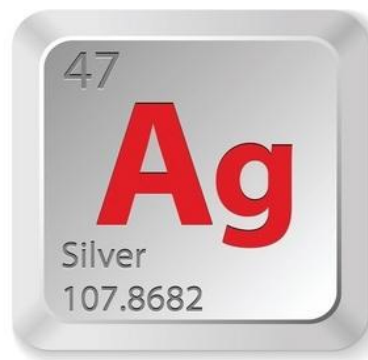
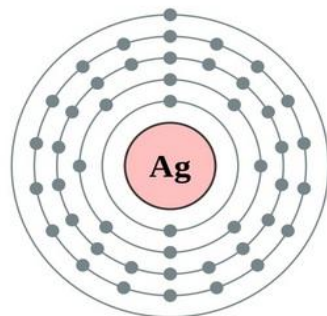
So if metals, which are usually used in their bulk form, are replaced with their nanostructures then many fold increase in the properties would be achieved.

1.3 Nobel metal nanomaterials (NMNs)

Nobel metals are those metals that either do not react or react to least extent with other elements. Pt, Pd, Ag and Au are some of the most common noble metals. At nano scale they have interesting physical and chemical properties. These are ideal building blocks for engineering and tailoring nanoscale structures for specific technological applications. Particularly, effectively controlling the size, shape, architecture, composition, hybrid and microstructure of NMNs plays an important role on revealing their new or enhanced functions and application potentials such as fuel cell and analytical sensors [5].

1.4 Silver

Silver is metallic, chemical element with the chemical symbol Ag, atomic number 47 and atomic weight 107.8682 g/mol. Ag is short form of the Latin word argentums (“arg” for “grey” or “shining”). It is a soft, white, lustrous transition metal having highest electrical and thermal conductivity. The metal occurs naturally in its pure, free form (native silver), as an alloy with gold and other metals, and in minerals such as argentite and chlorargyrite.



Silver has long been valued as a precious metal, and is used as an investment, to make ornaments, jewelry, high-value tableware, utensils, and currency coins. Silver is a very good conductor of electricity. Silver has the lowest contact resistance of any metal. Therefore, it is also used in electrical contacts and conductors. It is also used in mirrors and in catalysis of chemical reactions. Its compounds are used in photographic film. Dilute silver nitrate solutions and other silver compounds are used as disinfectants and micro biocides. Silver halides are photosensitive and are remarkable for their ability to record a latent image that can later be developed chemically.

Silver is stable in pure air and water, but tarnishes when it is exposed to air or water containing ozone or hydrogen sulfide. The most common oxidation state of silver is +1 (for example, silver nitrate, AgNO_3); the less common +2 compounds (for example, silver(II) fluoride, AgF_2), and the even less common +3 (for example, potassium tetrafluoroargentate(III), KAgF_4) and even +4 compounds (for example, potassium hexafluoroargentate(IV), K_2AgF_6) are also known.

1.5 Silver Nanoparticles

The size of silver nanoparticles is generally less than 100 nm in diameter. Ag NPs can be found in various shapes, such as sphere, cube, plate, octahedron, discs, rods, wires, stars, prisms and right bipyramids.

Out of these Nobel metals we use silver nanoparticles because of following reason:

- (1) Silver nanoparticles do not oxidized easily.
- (2) Ag nanoparticles are used because they are biocompatible.
- (3) Ag has been one of the most studied materials for nanostructures because of its superior performance in applications such as plasmonics and surface-enhanced Raman scattering (SERS) [6].

1.6 Applications of Silver Nanoparticles

Silver nanoparticles have found applications in textile engineering, water treatment, and silver-based consumer products. It has applications in catalysis, optics, electronics and other areas due to their unique size-dependent optical, electrical and magnetic properties.

1.6.1 Catalyst

Catalysis is modifies the rate of a chemical reaction. There are two types of catalyst:

(i) Homogeneous catalyst

(ii) Heterogeneous catalyst.

The reactants are distributed in the form of gas or liquid solution since; the homogeneous catalysts are in same phase. But heterogeneous catalysts are in a different phase so the reactants are separated by a phase boundary. Heterogeneous catalysts reactions usually take place on the surfaces of a solid catalyst [1]. In many applications silver nanoparticles are used as a catalyst [7-10]. Silver nanoparticles are used as catalyst for the bleaching of the organic dyes [11]. Silver nanoparticles catalyze the chemiluminescence from luminol–hydrogen peroxide system with catalytic activity better than Au and Pt colloid [12].

1.6.2 Textile industry

Silver nanoparticles are used in textile industry. Silver nanoparticles are used in cloths, socks etc, because of their antibacterial property. Silver nanoparticles can also reduce odor.

1.6.3 Medical uses

Silver nanoparticles are used as antibacterial or antifungal agents in biotechnology and bioengineering [13]. Silver nanoparticles are used to control the bacterial growth. Silver nanoparticles can be incorporated into a wide range of medical devices and wound dressings [14-17]. Silver nanoparticles have antibacterial activity used as a medicine to reduce the infection on skin burns [18]. The antimicrobial activities of silver nanoparticles are used in cotton dressings for burn wounds.

1.6.4 Water purification

Silver nanoparticles are used in water treatment because of their ability to remove pollution. It may be used in future at wide scale for water treatment [19].

1.6.5 Sensor

Silver nanoparticles are used in optical sensor having zeptomole (10^{-21}) sensitivity. Using the surface plasmon resonance effect, the silver nanoparticles gain a very high sensitivity [20]. Silver

nanoparticles are used as a sensor for H₂O₂ (Hydrogen peroxides) [21]. Silver nanoparticles are also used for ammonia sensing [22].

1.6.6 Electronics

Silver nanoparticles are used in electronics industry for circuit printing because silver has high conductivity [23].

1.6.7 Other useful applications

Silver nanoparticles are widely used as antibacterial/antifungal agents in variety of consumer products like air sanitizer sprays, pillows, slippers, respirators, wet wipes, detergents, soaps, shampoos, toothpastes, air filters, coatings of refrigerators, vacuum cleaners, washing machines, food storage containers, cellular phones, etc [24].

2.1 Synthesis of nanomaterials

Two approaches are used to fabricate metallic nanoparticles:

1. Top-down approach
2. Bottom-up approach

Both approaches are very important for synthesis of nanoparticles/ Nanostructures.

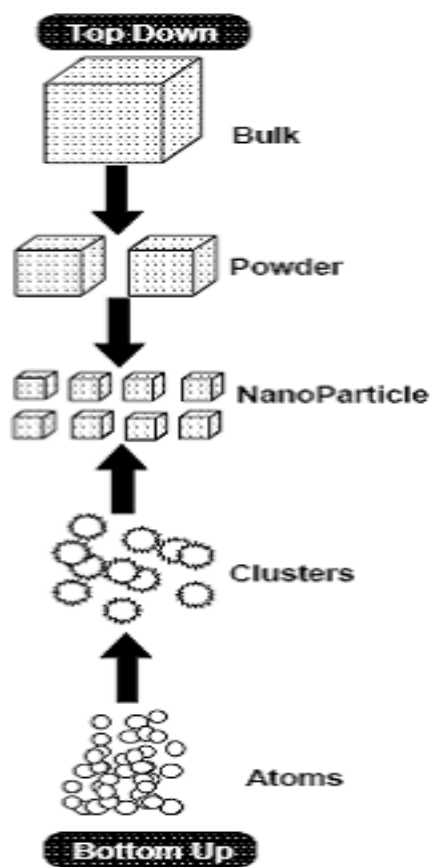


Figure 2.1: Schematic representation of the building up of nanostructures

2.1.1 Top-down approach

This approach refers to slicing or successive cutting of a bulk material to get nanoparticles or nanostructures. Examples of top-down are:

1. Attrition or Milling
2. Laser ablation
3. Sputtering
4. Etching
5. Vapor phase condensation
6. Electro-explosion

2.1.2 Advantages and disadvantages of top-down approach

The main problem with top-down approach is the imperfection of the surface structure. The conventional top-down techniques such as lithography can cause significant crystallographic damage. Additional defects may be introduced even during the etching steps. For example, nanowires made by lithography are not smooth and may contain a lot of impurities and structural defects on surface. These imperfections have significant impact on physical properties and surface chemistry of nanostructures and nanomaterials. Top-down approach also introduces internal stress, in addition to surface defects and contaminations.

Despite of these disadvantages the top-down approaches continue to play a significant role in the synthesis and fabrication of nanostructures because they are economical and mass scale production is possible with these methods.

2.1.3 Bottom-up approach

Bottom up approach refers to the buildup of a material from the bottom: atom by atom, or molecule by molecule or cluster by cluster.

Examples of bottom - up approach are:

1. Colloidal dispersion

2. Sol-gel
3. Nanolithography and nano manipulation
4. Micro-emulsion
5. Reverse micelle
6. Chemical co-precipitation
7. Chemical reduction

2.1.4 Advantages and disadvantages of bottom-up approach

Bottom-up approach promises a better chance to obtain nanostructures with less defects, more homogeneous chemical composition and better short and long range ordering. This is because the bottom-up approach is mainly driven by the reduction of Gibbs free energy, so that nanostructures and nanomaterials produced by these methods are in a state which is close to a thermodynamic equilibrium.

Some disadvantages of this approach are listed below:

- (1) Time consuming and tedious (complex).
- (2) It is difficult to maintain the temperature of mixture used for the synthesis of nanoparticles.
- (3) In this approach often undesirable results are obtained.

2.1.5 Difference between Top-down and Bottom-up approaches

1. In top-down approach manufacturing process starts from larger structures while in bottom-up approach starting building blocks are smaller than the final design.
2. Bottom-up manufacturing can produce structures with perfect surfaces and edges. Top-down manufacturing is not perfect as there are wrinkly or containing cavities.
3. Bottom-up approach manufacturing technologies are newer than top-down manufacturing and expected to be an alternative for it in some applications.
4. Bottom-up approach products have higher precision and therefore can manufacture smaller structures compared to top-down approach.

Li et al. [25] in 2005 demonstrated a facile synthesis of stable silver nanoparticles with a particle size of <10 nm. These nanoparticles were stabilized with easily detachable alkylamines, thus permitting their ready conversion at low temperatures to highly conductive silver elements suitable for low-cost, printed electronic applications. OTFTs with the printed silver source/drain electrodes of this nature exhibited TFT properties similar to those using vacuum-deposited silver electrodes.

Siekkinen et al. [26] in 2006, has described the fastest route to synthesize monodispersed silver nanocubes. By adding a trace amount of sodium sulfide (Na_2S) or sodium hydrosulfide (NaHS) to the conventional polyol synthesis. The reaction time was significantly shortened from 16–26 h to 3–8 min. It was found that by adjusting the reaction time, monodispersed silver nanocubes of 25–45 nm could be synthesized. These small nanocubes are of great interest for biomedical applications.

McLellan et al. [27] in 2006 synthesized sharp and truncated Ag nanocubes ranging from 60 to 100 nm in size. These nanoparticles were compared for surface-enhanced Raman scattering (SERS) activities with respect to both size and shape (i.e. sharp vs. truncated). They observed two trends: (i) larger particles (90 and 100 nm) were found to have higher SERS efficiencies, and (ii) particles with sharper corners gave more intense SERS signals than their truncated counterparts. The difference in enhancement factor was mainly attributed to the variation in overlap between the laser source and surface plasmon resonance (SPR) bands as a function of size and degree of truncation.

Chen et al. [28] in 2007 prepared nearly monodispersed silver nanoparticles in a simple oleylamine-liquid paraffin system. It was observed that the formation process of silver nanoparticles could be divided into three stages: growth, incubation, and Ostwald ripening stages. UV-visible spectroscopy, transmission electron microscopy (TEM) and high-resolution TEM have all demonstrated the occurrence of Ostwald ripening, which could result in better control over the size and size distribution of silver nanoparticles. Results showed that the as-obtained silver nanoparticles can self-assemble into ordered arrays. The possible reduction mechanism of silver ions by oleylamine is related to the Ag^+ mediated conversion of primary amines to nitriles.

Zhu et al. [29] in 2007, has reported effects of poly(vinyl pyrrolidone)/AgNO₃ ratio and temperature on the morphology and size of the products. Ag nanocubes with an average edge length of 230 nm were obtained successfully with sharp edges and corners under a precise synthesis condition. PVP played a critical role in directing the nucleation and growth of Ag nanocubes. The optical properties of Ag nanocubes show an attractive plasmon resonance. These nanocubes have potential applications in some areas such as SERS, chemical and biological sensing.

Li et al. [30] in 2009 used simple one-pot method to generate dimers of silver nanospheres in one step. The dimers consisted of single-crystal silver nanospheres have diameter~30 nm and with gap of 1.8 nm wide. They controlled the colloidal stability and oxidative etching by optimizing the amount of chloride added to the polyol synthesis. The dimers have well-defined system to study the hot spot phenomenon, an extremely important but poorly understood subject in surface-enhanced Raman scattering (SERS). Because of the relatively small size of the silver nanospheres, only those molecules which are trapped in the hot spot region are expected to contribute to the detected SERS signals. It was found by correlating SERS measurements with SEM imaging that the SERS enhancement factor within the hot spot region of such a dimer was of the order of 2×10^7 .

Chudasama et al. [31] in 2010 used a simple one pot method to produce uniform silver nanoparticles by thermal reduction of AgNO₃ using oleylamine as reducing and capping agent. Biocompatible block copolymer pluronic F-127 has been proved as a better alternative for facile phase transfer phenomenon to enhance the dispersal ability of as-synthesized hydrophobic silver nanoparticles in water, to retain their specific properties. Antimicrobial activities of hydrophilic silver nanoparticles is tested against two Gram positive (*Bacillus megaterium* and *Staphylococcus aureus*), and three Gram negative (*Escherichia coli*, *Proteus vulgaris* and *Shigella sonnei*) bacteria. Minimum inhibitory values were improved as compared to previously reported results which show that phase transferred silver nanoparticles are better antibacterial agents.

Xinping et al. [32] in 2011 tested antimicrobial activity and L-929 cell line was selected for toxicity evaluation by cellular mitochondrial function (MTT assay). They concluded that silver

nanoparticles can significantly increase antibacterial activity with increase in concentration of the silver nanoparticles. .

Zhao et al [33] in 2011 fabricated the titania nanotubes (TiO_2 -NTs) incorporated with silver (Ag) nanoparticles on Ti implants. They prepared Ag nanoparticles adhere tightly to the wall of the TiO_2 -NTs, by immersion in a silver nitrate solution followed by UV radiation. The amount of Ag introduced to the NTs could be varied by changing the AgNO_3 concentration and immersion time. The TiO_2 -NTs loaded with Ag nanoparticles (NT-Ag) could kill all the planktonic bacteria in the suspension during the first several days. The ability of the NT-Ag to prevent bacterial adhesion is maintained without obvious decline for 30 days, which was normally long enough to prevent post-operation infection in the early and intermediate stages and perhaps even late infection around the implant. Although the NT-Ag structure shows some cytotoxicity, it could be reduced by controlling the Ag release rate. The NT-Ag materials were also expected to possess satisfactory osteo conductivity in addition to the good biological performance expected of TiO_2 -NTs. This controllable NT-Ag structure which provides relatively long-term antibacterial ability and good tissue integration has promising applications in orthopedics, dentistry, and other biomedical devices.

Eminian et al. [34] in 2011 used silver nanoparticles photocurrent enhancement in thin film amorphous silicon solar cells. The light scattering properties of nanoparticles on glass and ZnO, and on silver coated with ZnO, which represent the back reflector of a solar cell, were studied. It was found that large nanoparticles embedded in the dielectric at the back contact of amorphous silicon solar cells lead to a remarkable increase in short circuit current by 20% compared to co-deposited cells without nanoparticles. This increase is strongly correlated with the enhanced cell absorption in the long wavelengths and is attributed to localized surface plasmon.

Panfilova et al. [35] in 2012, has investigated the influence of the parameters and conditions of sodium sulfide-induced reaction of polyol synthesis of silver nanoparticles on the yield of cube shaped particles. The optical properties of the colloids were also studied. The effect of reagent concentrations, degree of ethylene glycol oxygenation, and presence of impurities, reaction time, and temperature were also studied. It was found that suspensions containing nanoparticles with different shapes and sizes, including polydisperse particles of irregular shapes, silver nanocubes, and nanorods, can be produced by varying the synthesis parameters. The key parameters

controlling the yield of nanocubes were the degree of ethylene glycol oxygenation and the presence of trace amounts of ions of other metals.

Ahamad et al. [36] in 2012, demonstrated strategies for assembling silver nanocubes (NCs) into distinct 2D patterns on Langmuir–Blodgett (LB) films, using two different lipid mixtures as vehicles: (1) raft mixtures containing 1,2-dioleoyl-sn-glycero-3-phosphocholine (DOPC), sphingomyelin (SPM), and cholesterol in different mole ratios and (2) 1,2-dipalmitoyl-snglycero-3-phosphocholine (DPPC) and 1,2-dilauroylsn-glycero-3-phosphocholine (DLPC) at a 1:3 mol ratio. The results showed that aggregation of NCs into round-like pattern is governed by preferential localization of NCs within the liquid condensed (LC) domains of DOPC/SPM/Cholesterol mixture. First, circular islands of silver NCs (3 ± 1 μm in diameter) were observed in LB monolayer of DOPC/SPM/cholesterol mixed with silver NCs transferred at a lateral surface pressure of 10 m N/m.

Panfilova et al. [37] in 2012 prepared nanoparticles by galvanic replacement reaction between the Ag atoms of silver nanocubes and Au ions of tetra chloroauric acid. The particle plasmon resonance of Ag/Au ratio was tuned from 450 to 700 nm and the suspension color change from yellow to blue. The multiplex capability of the assay was illustrated by a proof-of-concept experiment involving simultaneous one-step determination of target molecules with a mixture of fabricated conjugates. Under naked eye examination, no cross-colored spots or non specific bioconjugate adsorption were observed.

Guzman et al. [38] in 2012 synthesized the Ag NPs by chemical reduction from aqueous solutions of silver nitrate, containing a mixture of hydrazine hydrate and sodium citrate as reductants and sodium dodecyl sulfate as a stabilizer. The characterization results of the SNPs show the agglomerates of grains with a narrow size distribution (from 40 to 60 nm). The radii of the observed particles were between the range 10 and 20 nm. They used Kirby-Bauer method to measure the antibacterial activity. The results showed reasonable bactericidal activity against *Escherichia coli*, *Pseudomonas aeruginosa*, and *Staphylococcus aureus*.

Chandni et al. [39] in 2012 studied the growth kinetics of ultrafine monodispersed silver nanoparticles prepared with the help of thermal reduction of silver nitrate with oleylamine. They monitor the effect of nucleation growth, temperature and time on the quality and quantity of silver nanoparticles in terms of product yield, crystal phase, morphology, aggregation, particle

size and size distribution. They observed that transformation of AgNO_3 into spherical Ag nanoparticles with simple cubic structure is mostly independent of kinetic parameters. They find best result for yielding of nanoparticles for 21 mM oleylamine. Its size decreases with increasing oleylamine concentration and levels off at 3.5 nm with a polydispersity of 0.12. When concentration of oleylamine is 15 mM, agglomerated silver nanoparticles resulted while they self-assembled into hexagonal close pack structure when oleylamine is 15 mM. Nucleation at 200°C for 30 min and growth at 150°C for 4 hr are the optimum processing parameters for highest nanoparticle yield (60%), lowest particle size (3.5 nm) and polydispersity index (0.12) with no or very little agglomeration.

3.1 Synthesis Method

There are many techniques available to synthesize different types of nanoparticles in the form of colloids, clusters powders etc. some methods are:

- (a) Biological method
- (b) Hybrid technique
- (c) Physical method
- (d) Chemical method

In nanoparticles synthesis, the difficult part is to control size, shape and morphology. In the present investigation the synthesis of silver nanocubes by chemical route is carried out and the nanocubes are characterized.

Chemical reduction methods have been widely investigated for the synthesis of silver nanoparticles because accuracy of process is better from the process requiring normal environmental conditions. These techniques can be executed under easy and gentle conditions, and can be used to synthesize silver nanoparticles on a large scale. The reducing capability of a reducing agent has a significant role in the synthesis of silver nanoparticles by the reduction reaction [40].

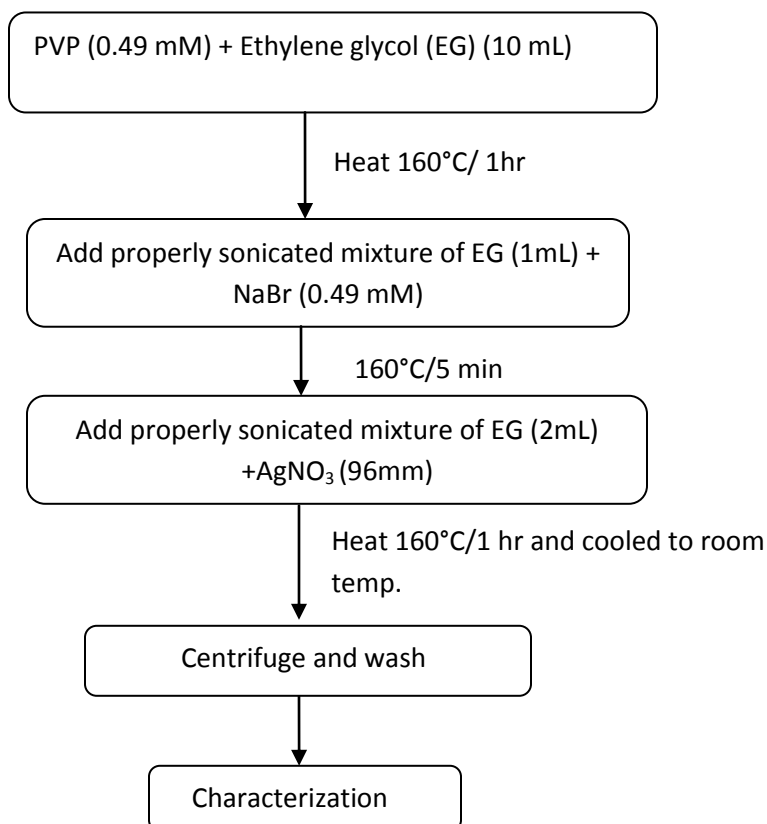
So we choose chemical reduction method to synthesize SNCs because it is easy and effective method to produce silver nanocubes as compare to other methods listed in bottom up approach. Silver nanostructures have been synthesized with a range of different shapes, including spheres, discs, rods, wires, stars, prisms, right bipyramids, and cubes [26]. Of these, single-crystal nanocubes appear to be the most exciting and useful structure particularly for the production of silver nanocubes that hold great promise for biomedical applications such as optical imaging contrast enhancement and photo thermal treatment [41].

3.2 Materials

The following materials and reagents were used in the work: silver nitrate, AgNO_3 (99.9%) was procured from s.d. fine-chem. Ltd as a precursor; ethylene glycol (99.8%), NaBr, PVP 10 was obtained from Sigma-Aldrich. Absolute ethanol was obtained from Merck. Ultrapure water was taken from a Milli Q system (specific resistance of $18 \text{ M}\Omega/\text{cm}$). All the chemicals were used as-received without any purification.

3.3 Synthesis of silver nanocubes

Silver particles were synthesized in a 250 ml three neck round bottom flask. The synthesis protocols are summarized in flow chart 3.1. The experimental setup used for the synthesis is shown in figure 3.1



Flow chart3.1: Synthesis protocol used to prepare silver nanocubes.



Figure 3.1: Experimental Setup used for the synthesis of Ag nanocubes.

3.4 Characterization Techniques

3.4.1 UV-visible Spectroscopy

Principle

The principle of UV-visible Spectroscopy is defined as when a beam of monochromatic light is passed through a solution of an absorbing substance, the rate of decrease of intensity of radiation with thickness of the absorbing solution is proportional to the incident radiation as well as the concentration of the solution. UV spectroscopy obeys the Beer-Lambert law, The expression of Beer-Lambert law is

$$\log(I_0/I) = \epsilon ck = A$$

Where, A is absorbance, I_0 is intensity of incident light, I is intensity of light leaving sample cell, c is molar concentration of solution (moles/litre), k is sample cell's length in cm and ϵ is molar absorptivity

From the Beer-Lambert law it is clear that greater the number of molecules capable of absorbing light of a given wavelength, the greater the extent of light absorption. UV-visible spectroscopy refers as absorption in the ultraviolet-visible spectral region. This means it uses light in visible and near UV and near-infrared regions. The absorption in the visible range directly affects the color of the chemicals involved. In the region of the e.m spectrum, molecules undergo electronic transitions. This method is complementary to fluorescence spectroscopy. The absorption of light occurs very fast at femto second time scale. The energy in a quantum is expressed by the Planck's law equation given below:

$$E = h\nu = hc / \lambda$$

Where E is the energy, h is Planck's constant, ν is the frequency, λ is the wavelength of incoming photon and c is the velocity of light.

Absorption of light is the one of the more useful instrumental method. The absorbance at a given wavelength by the compound shows the characteristics of its chemical structure. Absorption of visible and ultraviolet radiation is associated with excitation of electrons, in both atoms and molecules, to higher energy states. All the molecules undergo electronic excitation following, absorption of light for very high energy radiation is required. For molecules containing conjugated electron system, light in the UV-visible region is adequate.

Instrumentation

The basic parts of a spectrophotometer are light source, a holder for the sample, a diffraction grating or monochromator and a detector. The construction of traditional UV-visible spectrometer is similar to an IR spectrophotometer. Schematic representation of UV-visible spectrophotometer is shown in figure 3.2

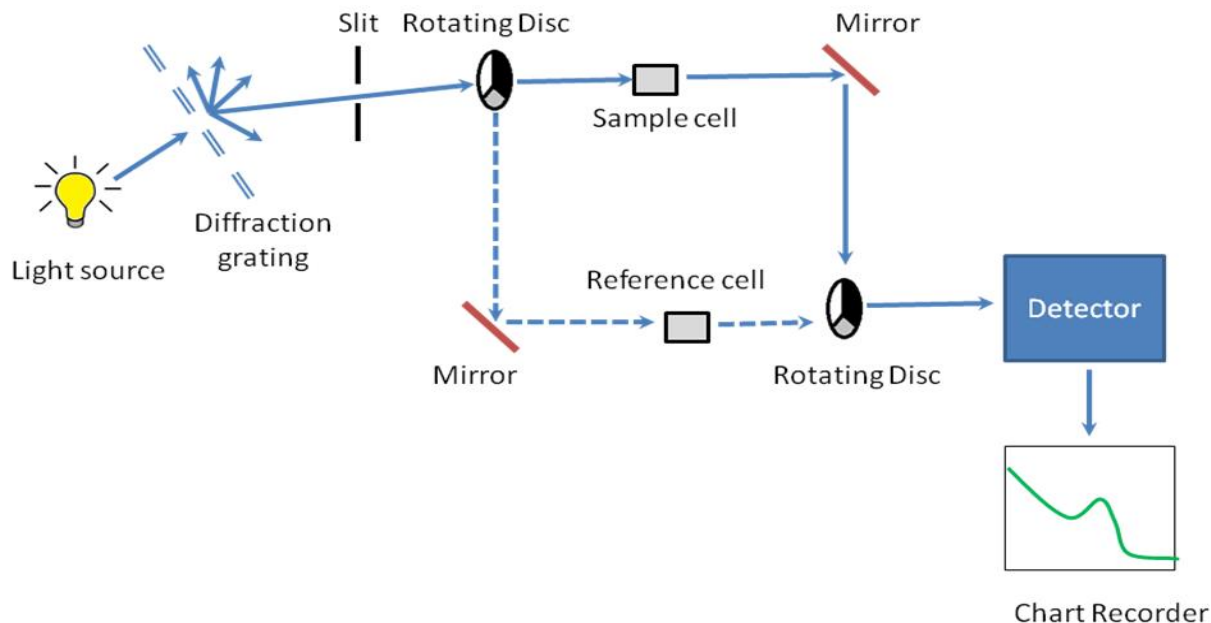


Figure 3.2: Schematic ray diagram of UV visible spectrophotometer

UV spectroscopy is used to obtain the absorbance spectra of a compound in solution or as a solid. UV-visible spectroscopic data can give qualitative and quantitative information of a given compound or molecule. Optical properties of metal and metal oxide nanoparticles will be evaluated by UV-visible spectroscopy.

Applications of UV-visible spectroscopy

- UV-visible spectroscopy is used to detect the impurity or purity of the compound.
- UV-visible spectroscopy can characterize those type of compounds which absorb UV-radiation. Kinetics of the reaction can also be studied using UV-Spectroscopy.
- This technique is used to detect the presence or absence of the functional group in the Compound.

3.4.2 X-Ray Diffraction

Principle

X-ray diffraction is based on constructive interference of monochromatic X-rays and a crystalline sample. X-rays are generated by a cathode ray tube, filtered to produce

monochromatic radiation, collimated to concentrate, and directed toward the sample. The interaction of the incident rays with the sample produces constructive interference when conditions satisfy the Bragg's Law get satisfied.

A typical powder XRD instrumentation consist of four main components such as, X-ray source, specimen stage, receiving optics and X-ray detector. The source and detector with its associated optics lie on the circumference of focusing circle and the sample stage at the centre of circle. The angle between the plane of the specimen and the X-ray source is θ , known as Bragg's angle and angle between the projections of X-ray source is 2θ .

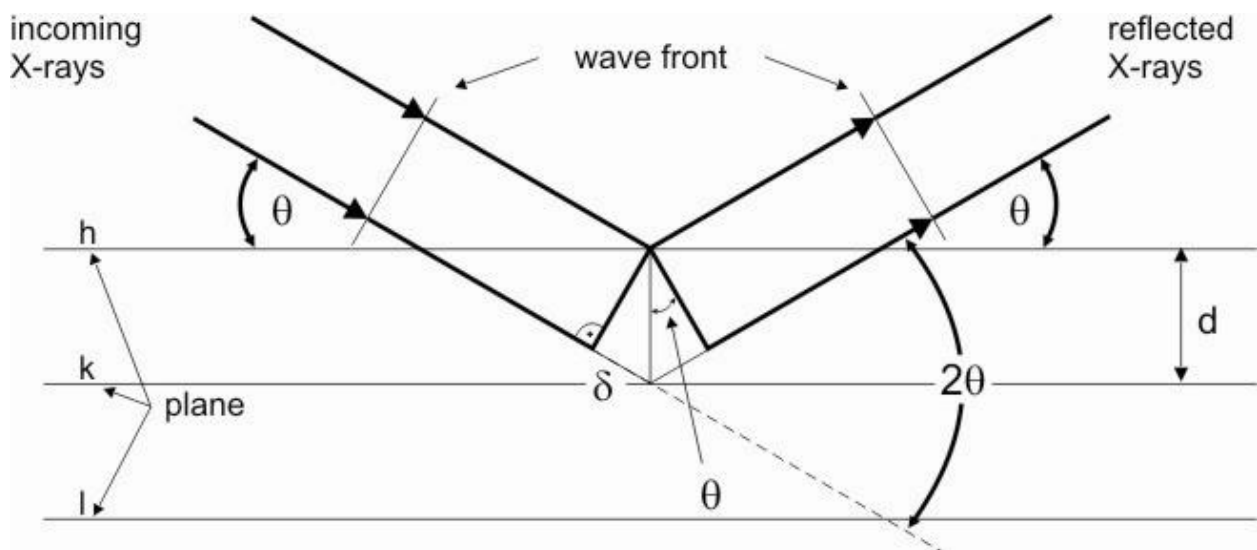


Figure 3.3: Principle of X-ray diffraction.

Working

For the XRD analysis, fine powder was mounted on the sample holder and the powder was assumed to consist of randomly oriented crystallites. When a beam of X-ray is incident on the sample, X-ray are scattered by each atom in the sample. If the scattered beams are in phase, these interfere constructively and one gets the intensity maximum at that particular angle. The atomic planes from where the X-ray are scattered are referred to as reflecting planes. So, X-ray diffraction yields the atomic structure of materials and is based on the elastic scattering of X-rays from the electron clouds of the individual atoms in the system.

Application

By using XRD we can measure

- The crystal structure,
- d-spacing,
- Lattice parameter,
- Strain,
- Crystallite size of the particles,
- Thin film thickness,

3.4.3 Transmission electron microscope

Transmission electron microscopy (TEM) is used to obtain information from samples that are thin enough to transmit electron. In TEM, the whole area of observation is illuminated using an electron source of adequate intensity. The transmitted electrons are generally used to form either an image or a diffraction pattern of the specimen. The formation of image and electron diffraction in TEM can be understood from schematic ray diagram as shown in figure 3.4. When a crystal of lattice spacing 'd' is illuminated with electrons of wavelength ' λ ', the diffracted waves will be produced at specific angles, 2θ for $n = 1$, satisfying the Bragg's condition $2d \sin\theta = n\lambda$. The diffracted waves form diffraction spots on the back focal plane. In an electron microscope, the use of electron lenses allows the regular arrangement of diffraction spots to be projected on a screen and the electron diffraction pattern can be observed.

If the transmitted and the diffracted beam interfere on the image plane, a magnified image can be observed. The space where the diffraction pattern forms is called the reciprocal space, while the space at the image plane or at a specimen is called the real space. In TEM, by adjusting the electron lenses, both the microscope images and diffraction patterns can be observed. Thus in the analysis of microstructures of materials, both observation modes can be successfully combined. In an investigation of electron diffraction pattern, the electron microscope images of the nano phosphor is first observed of the whole area and then by inserting an aperture in a specific area and adjusting the electron lenses a diffraction pattern

of the area is obtained. The latter observation mode is called selected area electron diffraction (SAED).

Because SAED can be obtained from each grain, the crystal structure and mutual crystal orientation relationship between adjacent grains can easily be clarified. The observational dimension selected from the object is usually limited to about 0.1 micrometer in diameter. However, in micro diffraction method, the diffraction pattern can be obtained from an area correspondingly to only a few nanometers in diameter. Then, by passing the transmitted beam or one of the diffracted beams through an aperture and changing to the imaging mode, the image with enhanced contrast can be observed. The observation mode using the transmitted beam is called the bright field method, and the image observed is a bright field image.

Instrumentation

The TEM have several components, they are vacuum system in which the electrons travel, an electron emission source for generation of the electron stream, a series of electromagnetic lenses as well as electrostatic plates. The latter two allow the operator to guide and manipulate the beam as required.

Applications

TEM is used for following purposes:

- Electron diffraction studies,
- Morphological analysis,
- Crystallographic information of the sample.

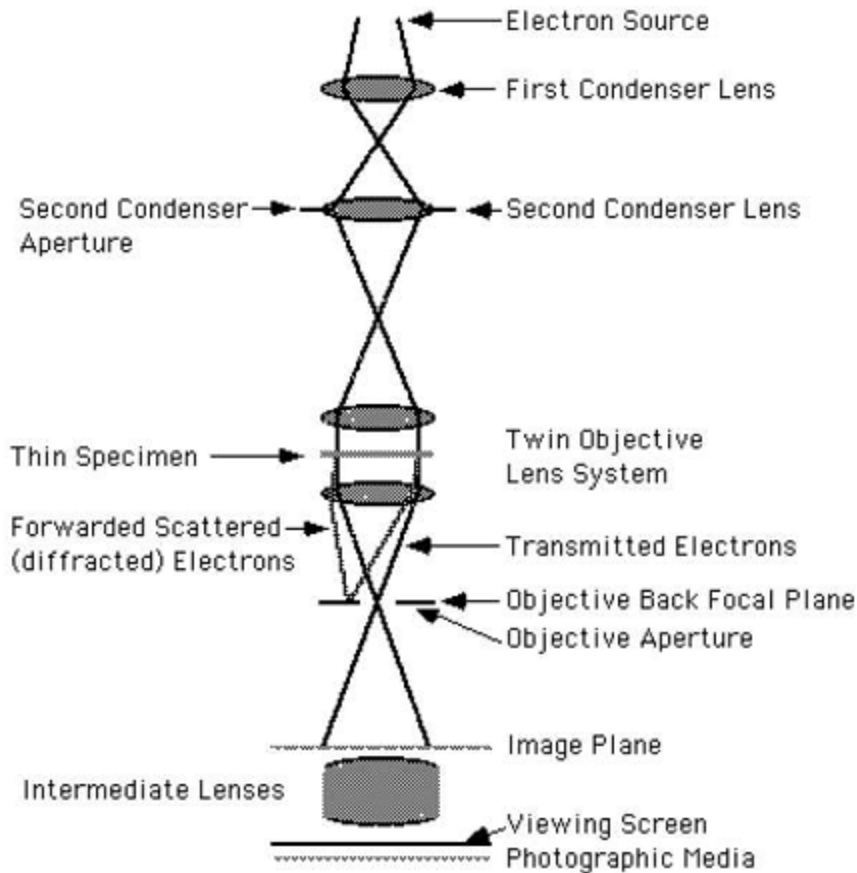


Figure 3.4: Schematic ray diagram of TEM.

3.4.4 Dynamic Light Scattering (DLS)

Dynamic light scattering is also known as photon correlation spectroscopy. This is used to determine the size distribution profile of small particles in suspension or polymers in solution. It can also be used to probe the behavior of complex fluids such as concentrated polymer solutions. When light hits small particles, the light scatters in all directions (Rayleigh scattering) as long as the particles are small compared to the wavelength (below 250 nm). If the light source is a laser, and thus is monochromatic and coherent, then one observes a time-dependent fluctuation in the scattering intensity. This fluctuation is due to the fact that the small molecules in solutions are undergoing Brownian motion, and so the distance between the scatter in the solution is constantly changing with time. This scattered light then undergoes either constructive or destructive interference by the surrounding particles, and within this intensity fluctuation, information is contained about the time scale of movement of the scatter.



Figure 3.5: Brookhaven's 90 plus particle size analyzer.

Sample preparation either by filtration or centrifugation is critical to remove dust and from the solution. DLS is used to characterize size of various particles including proteins, polymers, micelles, carbohydrates, and nanoparticles. If the system is monodisperse, the mean effective diameter of the particles can be determined. This measurement depends on the size of the particle core, the size of surface structures, particle concentration and the type of ions in the medium.

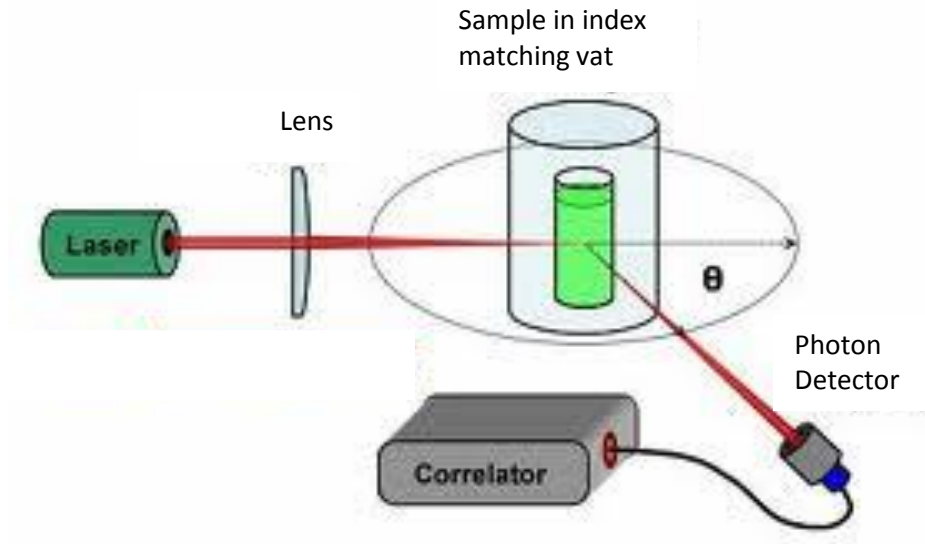


Figure 3.6: Schematic diagram of particle size analyzer.

DLS essentially measures fluctuations in scattered light intensity due to diffusing particles, the diffusion coefficient of the particles can be determined. DLS software of commercial instruments typically displays the particle population at different diameters. If the system is monodispersed, there should only be one population, whereas a polydisperse system would show multiple particle populations.

Applications of DLS

- Used to determine the size and size distribution (polydispersity).
- The mean effective diameter of the particles is calculated.
- The diffusion coefficient of particles can be determined by DLS.
- DLS is also used to determine the stability of the sample.

3.4.5 Thermal Gravimetric Analysis (TGA)

Thermo gravimetric analysis or thermal gravimetric analysis (TGA) is a method of thermal analysis in which the changes in physical and chemical properties of materials are measured as a function of temperature or time. TGA can provide information about physical phenomena, such as vaporization, sublimation, absorption, adsorption, and desorption. Chemisorptions, decomposition, and solid-gas reactions (e.g., oxidation or reduction). Some materials can gain

weight by reacting with the atmosphere in the testing environment. Since weight loss and gain are disruptive processes to the sample material or batch, knowledge of the magnitude and temperature range of those reactions are necessary in order to design adequate thermal ramps and holds during those critical reaction periods. It is a type of testing that is performed on samples to determine changes in weight in relation to change in temperature. Such analysis relies on a high degree of precision in three measurements: weight, temperature, and temperature change. As many weight loss curves look similar, the weight loss curve may require transformation before results may be interpreted. A derivative weight loss curve can be used to tell the point at which weight loss is most apparent. Again, interpretation is limited without further modifications and deconvolution of the overlapping peaks may be required. TGA is commonly employed in research and testing to determine characteristics of materials such as polymers, to determine degradation temperatures, absorbed moisture content of materials, the level of inorganic and decomposition points of explosives and solvent residues. It is also often used to estimate the corrosion kinetics in high temperature oxidation.



Figure 3.7: NETZSCH TGA/DTA thermal analyzer.

Some common applications of TGA are:

- Used to study the absorption surfaces including with the nature and process involved in thermal decomposition,
- Studies Thermal and oxidation stability of materials
- Determination of organic content in a sample, and
- Determination of inorganic (e.g. ash) content in a sample, which may be useful for corroborating predicted material structures or simply used as a chemical analysis.
- Decomposition kinetics of the materials, It is an especially useful technique for the study of polymeric materials, including thermoplastics, thermosets, elastomers, composites, plastic, fills, fibers, coatings and paints.

4.1 UV- visible Spectroscopy

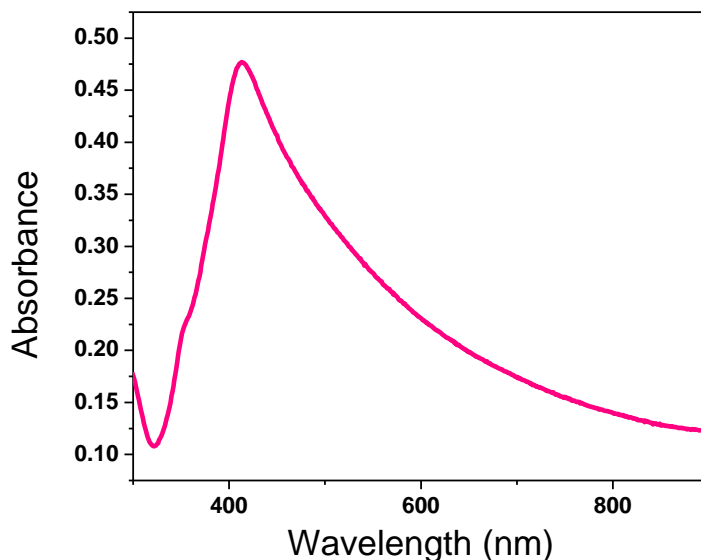


Figure 4.1: UV- visible spectra of Ag nanocubes.

Figure 4.1 shows the UV- visible spectra of Ag nanocubes. UV-Vis spectra of silver nanocubes dispersed in deionized water were recorded at room temperature on Anaytikjena specord-205 UV-visible spectrometer. Strong surface plasmon resonance peaks is observed at 412 nm. The asymmetric nature of this absorption hints towards the formation of non spherical nanostructure. According to Mie's theory multiple surface resonance peaks should be observed in case of non-spherical noble metals nanostructure. The presence of a sharp hump just below 400 nm, confirms the formation of silver nanocubes. Similar observation was reported by large number of groups, the broadness of the peak also hints toward the higher polydispersity in the size of silver nanocubes.

4.2 XRD

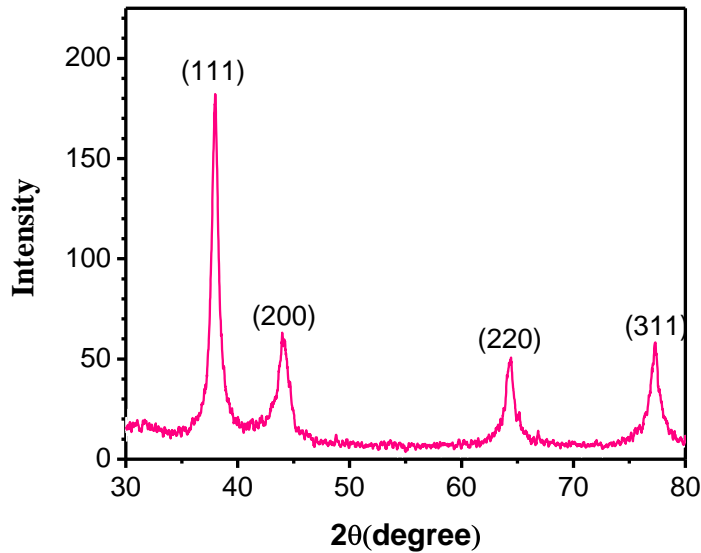


Figure 4.2: X-ray diffraction pattern of silver nanocubes.

Figure 4.2 shows the XRD pattern of silver nanocubes which are recorded on PANalytical X'pert PRO with $\text{CuK}\alpha$ ($\lambda=1.5418\text{\AA}$). The XRD pattern matches the face-centered cubic (fcc) structure with (111), (200), (220) and (311) planes corresponding to the angle (2θ) at 38.2° , 44.1° , 64.4° and 77.2° respectively. The observed spectra are also matching with the standard JCPDF diffraction database card no. **040783**. The line broadening of XRD peaks shows the particles of nano size. The average crystalline size (D) of silver nanocubes has been calculated, by using Debye-Scherrer formula.

$$D = 0.9 \lambda / \beta \cos\theta$$

Where λ is characteristics wavelength used (1.5406\AA), β is the full width at half maxima

(FWHM) of diffraction peaks and θ is Bragg's angle.

Table 4.1: Crystallite size obtained from various diffraction peaks.

Crystal plane	Θ (rad)	β (rad)	Size (nm)
(111)	0.33140	0.0110	12.60
(200)	0.38460	0.0171	8.11
(220)	0.56135	0.0155	8.95
(311)	0.67430	0.01761	7.87

The average size is 9.38 nm.

d- Spacing values were calculated by using Bragg's law i.e. $2d \sin\theta = n \lambda$ and values were given below in Table 4.2

Table 4.2: Calculated d-spacing corresponding to each Bragg's reflection.

S. No.	Crystal Plane	d- spacing(nm)
1	(111)	0.24
2	(200)	0.21
3	(220)	0.15
4	(311)	0.12

Silver nanoparticles have fcc structure ($a=b=c$, $\alpha=\beta=\gamma=90^\circ$), to calculate the value of lattice parameter we use the

$$1/d_{hkl}^2 = h^2 + k^2 + l^2 / a^2$$

Table4.3: Lattice parameter of silver nanocubes.

S. No	Crystal plane	Lattice parameter (Å)
1	(111)	4.08
2	(200)	4.08
3	(220)	4.08
4	(311)	4.08

The average lattice parameter is 4.08 Å.

The observed values of crystallite size, inter planner spacing and Lattice parameter are good agreement with phase reported in the literature.

4.3 TEM

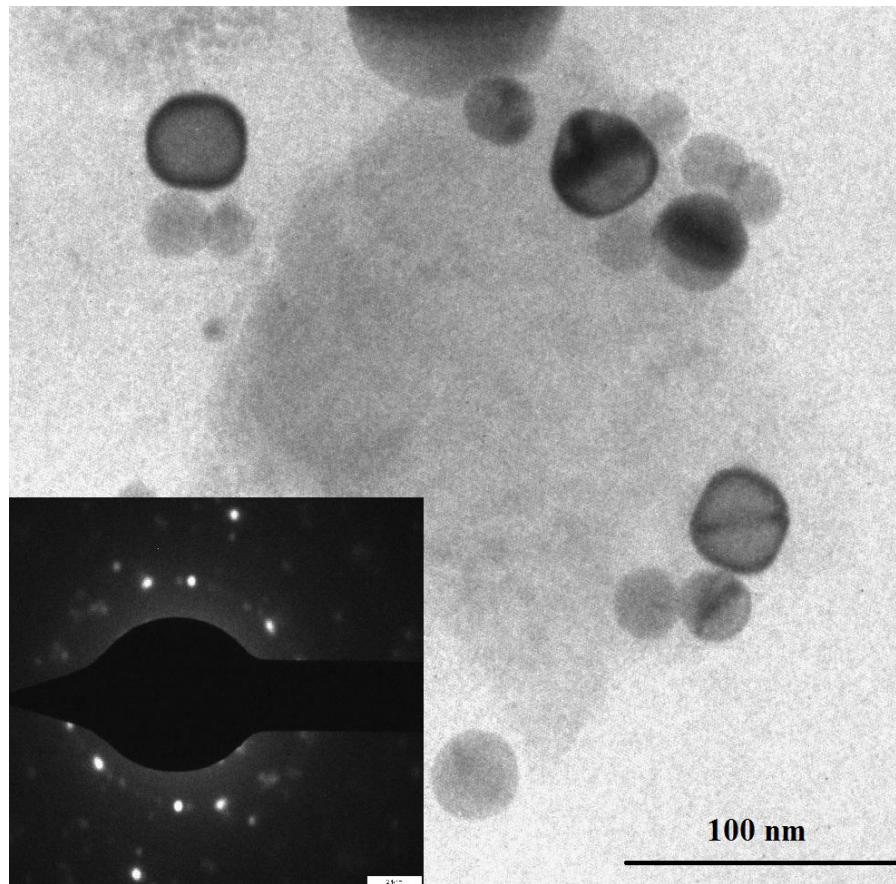


Figure 4.3: TEM image of silver nanocubes inset shows the electron diffraction images of Ag nanocubes.

Figure 4.3 shows the transmission electron microscopic image of as-synthesized silver nanocubes. The edge length was found to be 30 nm. The presences of few spherical silver nanoparticles are also observed the electron diffraction image of silver is also in good agreement with the X-ray diffraction results explained in Table 4.2.

4.4 Dynamic Light Scattering (DLS)

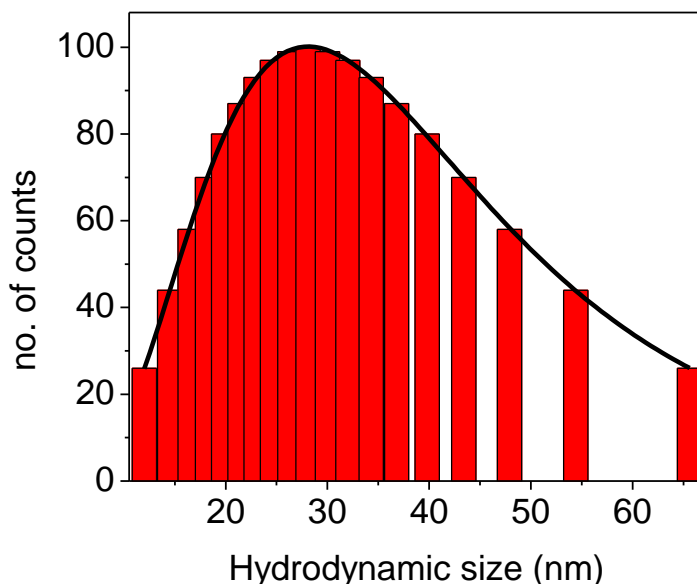


Figure 4.4: Hydrodynamic size distribution of silver nanocubes.

Figure 4.4 shows the hydrodynamic particle size distribution of silver nanocubes. Particle size distribution analysis was carried out on Brookhaven's DLS model. Hydrodynamic size of silver nanocubes was observed to be 36.4 ± 0.16 nm with polydispersity index of 0.5. The size of silver nanocubes comes out to be high because, it is the size of nanocubes and the size of the coating of PVP 10 polymer. The results are in agreement with the transmission electron microscopy result.

4.5 Thermo gravimetric Analysis

From the Figure 4.5 it is clear that up to 650°C there is negligible weight loss was observed. But on further increasing the temperature a large weight loss is observed up to 900°C . Above this temperature the mass of sample was found to be constant. After calculation it was observed that the total weight loss is 42.53%. This weight loss corresponds to the evaporation of PVP 10 from the surface of nanocubes. This mass of PVP 10 is necessary to prevent agglomeration between silver nanoparticles.

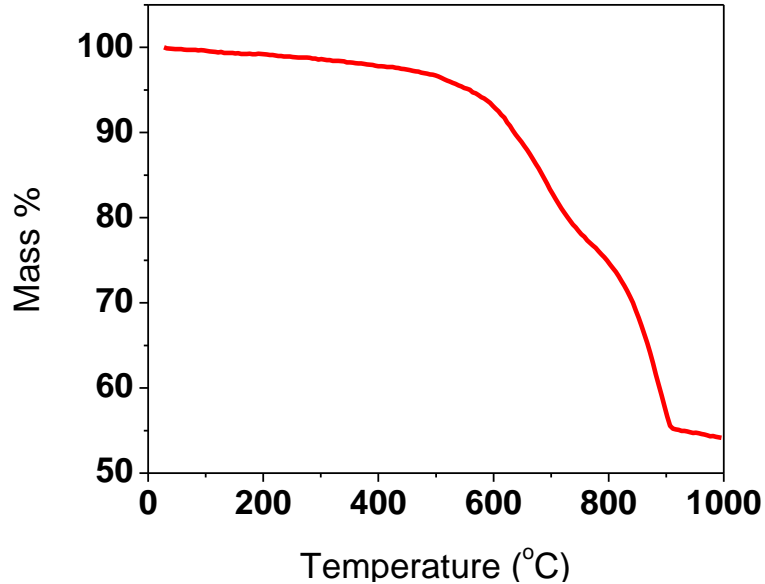


Figure 4.5: TG curve of Ag nanocubes.

Conclusions

- **Silver nanocubes** have prepared by **polyol process**.
- XRD confirms the **face centred cubic (fcc)** phase silver nanocubes.
- The average crystalline size of the silver nanoparticles obtained from the peak broadening of diffraction peak was **9.38 nm**.
- **UV-Visible spectrum** of the sample, hints toward the **cubic shape** of the silver nanoparticles, which further confirmed by **transmission electron microscopy**.
- The presence of **PVP coating** is confirmed through **TG analysis**. This coating of PVP prevents the agglomeration of nanoparticles.

REFERENCES

- [1] C. P. Poole Jr. and F. J. Owens, Introduction to Nanotechnology, John Wiley & Sons, Inc., Hoboken, New Jersey (2003).
- [2] L. filipponi and D. Sutherland, Nanotechnology-brief introduction .2007.
- [3] N. Lane, J Nano.res.3 (2005) 95
- [4] N. Lubick, Environ Sci Techno 42 (2008) 11
- [5] S. Guo, E. Wang, Nano Today 6 (2011) 240
- [6] A.R. Siekkinen, J.M. McLellan, J. Chen, Y. Xia, Chemical Physics Letters 432 (2006) 491
- [7] Z. J. Jiang, C. Y. Liu, and L. W. Sun, Journal of Physical Chemistry B, 109 5 (2005) 1730
- [8] K. Tsujino, M. Matsumura, Adv. Matterials 17 8 (2005) 1045
- [9] R. J. Chimentão, I. Kirm, F. Medina, X. Rodríguez, Y. Cesteros, P. Salagreb, J. E. Sueiras Chem. Commun. (2004) 846
- [10] A. C. Patel, S Li, C. Wang, W. Zhang, Y. Wei, Chem. Mater.19 (2007) 1231
- [11] J. Kohler, L. Abahmane, J. Albert, G. Mayer, Chem. Eng. Sci. 63 (2008) 5048
- [12] J. Guo, H. Cui, W. Zhou, W. Wang, J.Photochem. Photobiol. A. Chem 193 (2008) 89
- [13] M. K. Shukla, R. P. Singh, C.R.K. Reddy, B. Jha, Bioresource Technology 107 (2012) 295
- [14] M. Bosetti, A. Masse, E. Tobin, M. Cannas, Biomaterials 23 3 (2002) 887
- [15] M. Cho, H. Chung, W. Choi, J. Yoon, Appl. Environ. Microbiol. 71 1 (2005) 270
- [16] A. Gupta, S. Silver, Nat. Biotechnol. 16 (1998) 888
- [17] Q. Li, S. Mahendra, D. Lyon, L. Brunet, M. Liga, D. Li, P. Alvarez, Water Res. 42 (2008) 4591
- [18] E. Ulkur, O. Oncul, H. Karagoz, E. Yeniz, B. Celikoz, Burns 31 (2005) 874
- [19] P. Jain, T. Pradeep, Biotechnol. Bioeng. 90 1 (2005) 59
- [20] A.D. Mcfarland, R.P.V. Duyne, Nano Letters 3 (2003) 1057
- [21] A.Kulkarni, S.R. Dugasani, R. Aiyer, S.Park, A. Kulkarni, S. Sabharwal, Sensor and Actuators B 183 (2013) 144
- [22] S.T. Dubas, V. Pimpan, Talanta 76 (2008) 29
- [23] Y. Li, X. Wu, B.S. Ong, J Am Chem Soc 127 (2005) 3266
- [24] C. Buzea, I. I. Pacheco, K. Robbie, Biointerphases 2 (2007) 17
- [25] Y. Li, Y. Wu, B. S. Ong, J. Am. Chem. Soc. 127 (2005) 3266
- [26] A.R. Siekkinen, J.M. McLellan, J. Chen, Y. Xia, Chemical Physics Letters 432 (2006) 491

- [27] J. M. McLellan, A. Siekkinen, J. Chen, Y. Xia, Chem. Phys. Lett. 427 (2006) 122
- [28] M. Chen, Y.G.Feng, X.Wang, T. C. Li, J. Y. Zhang, D. J. Qian, Langmuir 23 10 (2007) 5296
- [29] J. Zhu, C. Kan, X. Zhu, J. Wan, M. Han, Y. Zhao, B. Wang, G. Wang, J. Mater. Res., 22 6 (2007) 1479
- [30] W. Li, P. H. C. Camargo, X. Lu, Y. Xia, Nano Letters 9 1 (2009) 485
- [31] B. Chudasama, A. K. Vala, N. Andhariya, R. V. Mehta, R. V. Upadhyay, J Nanopart Res., 2010
- [32] L. Xinping, L. Shengli, Z. Miaotao, Z. Wenlong, L. Chuanghong, Rare Metal Mater. Eng. 40 (2011) 209
- [33] L. Zhao, H. Wang, K. Huo, L. Cui, W. Zhang, H. Ni, Y. Zhang, Z. Wu, P. K. Chu, Biomaterials 32 (2011) 5706
- [34] C. Eminian, F.-J. Haug, O. Cubero, X. Niquille, C. Ballif Prog. Photovolt: Res. Appl. 19 (2011) 260
- [35] E. Panfilova, A. M. Burov, N. G. Khlebtsov, L. Matora, Colloid Journal, 74 1 (2012) 99
- [36] N. Ahamad, D. Prezgot, A. Ianoul, J Nanopart Res. 14 (2012) 724
- [37] E. Panfilova, A. Shirokov, B. Khlebtsov, L. Matora, N. Khlebtsov, Nano Res. 5 2 (2012) 124
- [38] M. Guzman, J. Dille, S. Godet, Nanomedicine: Nanotechnology, Biology, and Medicine 8 (2012) 37
- [39] Chandni, N. Andhariya, O.P. Pandey, B. Chudasama, RSC Adv., 3 (2012) 1127
- [40] U. T. Khatoon, K. V. Rao, J.V.R. Rao, Y.Aparna, IEEE (2011) 97
- [41] J. Chen, F. Saeki, B. Wiley, H. Cang, M. Cobb, Z. Li, L. Au, H.Zhang, M. Kimmey, X. Li, Y. Xia, Nano Lett. 5 (2005) 473

